

# Analysis and Design of Adaptive Self-Trimming Technique For A/D Converters

Zhiqiang Gu†  
*Bell-Northern Research Ltd.*  
*P.O.Box 3511, Station C*  
*Ottawa, Ontario, Canada K1Y 4H7*  
*Telephone: (613) 765-3580*  
*Fax: (613) 763-2626*  
*Email: ggu@bnr.ca*

W. Martin Snelgrove†  
*Dept. of Electronics*  
*Carleton University*  
*Ottawa, Ontario, Canada K1S 5B6*  
*Telephone: (613) 788-2381*  
*Fax: (613) 788-5708*  
*Email: snelgar@keiko.doe.carleton.ca*

†*Previously with Dept. of Electrical and Computer Engineering, University of Toronto,  
Toronto, Ontario, Canada M5S 1A4*

**TOPIC: CIRCUITS AND SYSTEM THEORY OR ANALOG CIRCUITS AND FILTERS**

## ABSTRACT

A novel self-trimming algorithm for A/D converters [1,2] has been presented which continually trims thresholds in the flash A/D subconverters of two-stage and pipelined A/D converters. Roughly speaking, it trims thresholds up or down by small increments in such a way as to smooth out irregularities in the code density. This paper presents the mathematical analysis and design of the algorithm. The algorithm was analyzed by a novel two-dimensional z-transform introduced in [3], which can be used to demonstrate its stability, predict convergence rate, and which can be used to give a frequency-domain interpretation of the distinct properties of differential and integral nonlinearity.

## I. INTRODUCTION

The self-trimming algorithm in the self-calibration technique for two-stage and pipelined A/D converters presented in [1,2] is histogram-based, because the histogram of digital output codes from an A/D converter offers information on all bit transition levels and so allows us to monitor the linearity of the A/D converter [4]. The critical problems that we have solved in using the histogram-based information further for threshold adaptation in A/D subconverters of a multi-stage A/D converter are: (1). how to derive the code histogram; and (2). what reference this histogram can be compared to.

In this paper we describe mathematically the mechanism of the self-trimming algorithm, and then present a frequency-domain analysis using a 2-D z-transform introduced in [3] for A/D converter nonlinearity.

## II. HISTOGRAM-BASED SELF-TRIMMING ALGORITHM

For a flash A/D converter shown in Fig.1, the histogram of digital codes resulting from the converter can be plotted as in Fig.2, where on the horizontal axis the input signal  $v_{in}$  defines the voltage scale (in volts) and an array of comparator thresholds  $x_i, i = 1, \dots, 2^N - 1$  ( $N$  is the resolution of this A/D converter) spread out along the axis; each pair of adjacent thresholds outlines a quantitative interval, and the height of the interval represents occurrences of digital output codes falling into this interval. Because the thermometer codes which come out immediately from the comparator array don't give unambiguous code information for our histogram calculation, only codes  $b_i$  from the latch-bank circuit which follows the comparator array (see Fig.1) will be concerned hereafter for the rest of this paper.

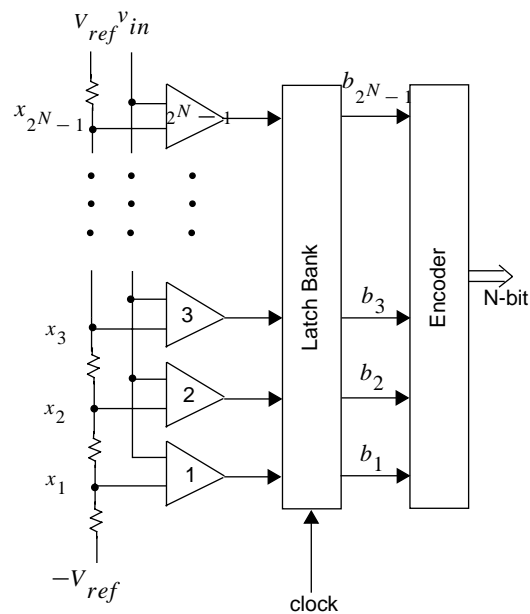


**Fig.1 Block diagram of an N-bit flash A/D converter**

The first case that we consider before going into the detail of the self-trimming algorithm is that there exists

an analog input signal  $v_{in}$  to an ideal flash A/D converter which can give a set of digital output codes at the converter's output, and these digital codes have a nearly-uniform code histogram. The nearly-uniform histogram is represented as a horizontal dashed line in Fig.2. Mathematically, the identity of the histogram can be described as: the histogram value  $p(i)$  of  $i$ -th interval  $\approx$  constant  $h$  for  $i = 1, \dots, 2^N$ . Therefore,  $p(i)$  can be expressed as:

$$p(i) = \int_{x_{i-1}}^{x_i} \rho(x') dx' \quad (1)$$

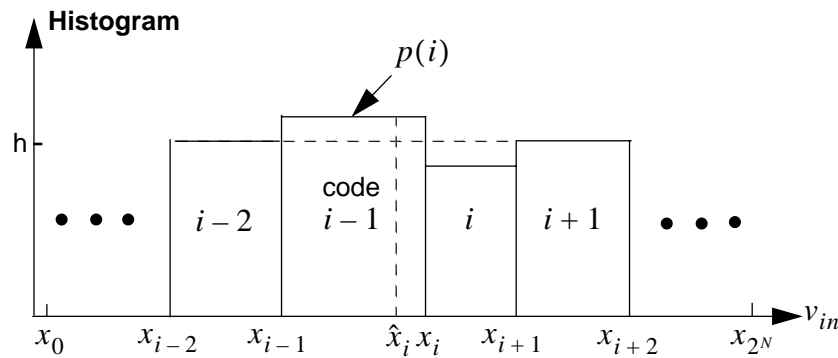


**Fig.2 Histogram of input signal  $v_{in}$  and digital output codes**

where  $\rho(x')$  is the probability density function of  $x' \in [x_{i-1}, x_i]$ , and two boundary conditions for the equation are  $x_0 \equiv 0$  and  $x_{2^N} = V_{ref}$  ( $V_{ref}$  is the reference voltage of the A/D converter shown in Fig.1).

Note that these two boundary conditions are set by the limit of the converter's conversion range but are not associated with any physically-existing comparator thresholds. In fact, they are equivalent to  $x_0 \equiv -\infty$  and  $x_{2^N} \equiv \infty$ , respectively, since in reality output codes which fall outside  $[0, V_{ref}]$  will be assigned codes 0

or  $2^N - 1$  which actually belongs to the two end quantization intervals  $[0, x_1)$  and  $[x_{2^N-1}, V_{ref}]$ . For

a uniform sampling over a full conversion range, i.e.,  $[0, V_{ref}]$ ,  $\rho(x)$  is approximately a constant  $\rho$  for all

$x \in [0, V_{ref}]$  under the assumption about the input signal  $v_{in}$  given above. In this case, Eq.(1) can be simplified as:

$$p(i) \approx \rho \cdot (x_i - x_{i-1}), i = 1, \dots, 2^N \quad (2)$$

Now let us consider another case where the flash A/D converter is nonideal and then see how our self-trimming algorithm works when some out of  $2^N - 1$  comparator thresholds is offset for some reasons. Fig.2 shows such a case by solid lines where the error-contaminated threshold  $x_i$  is greater than its desired value  $\hat{x}_i$  (these two values are represented as a vertical solid line and a vertical dashed line, respectively). Then we have a distorted histogram in which the histogram interval  $[x_{i-1}, x_i)$  to the left of  $x_i$  has a height higher than the desired value  $h$ , i.e., more samples fall into this interval because a larger  $x_i$  increases the chance of receiving codes. Accordingly, the histogram interval  $[x_i, x_{i+1})$  to the right of  $x_i$  has a height lower than  $h$ , because the chance of samples' falling into this interval is decreased.

There are probably many ways to reduce the chance of samples' falling into  $[x_{i-1}, x_i)$  and meanwhile to increase the chance for  $[x_i, x_{i+1})$  by trimming the comparator thresholds. The mandatory requirement for any feasible approach is that at least the cumulative effect of the threshold trimming at equilibrium must be that these two heights are smoothed out, and the entire histogram is close to uniformity so that it gives a nearly-uniform spacing of all the thresholds. Another reasonable requirement is that the corresponding trim circuitry use the existing output codes, if at all possible, rather than needing new codes which cost extra circuitry.

Our solution for the self-trimming, which was proposed and developed in this research, meets these requirements. Mathematically, it is simply described as:

For each individual quantization interval, e.g.,  $i$ -th interval where  $i \in [1, 2^N]$ ,

$$\begin{aligned} &\text{if } x_{i-1}(t) \leq v_{in}(t) < x_i(t) , \\ &x_{i-1}(t+T) = x_{i-1}(t) + \Delta ; x_i(t+T) = x_i(t) - \Delta . \end{aligned} \quad (3)$$

with two end conditions:  $x_0(t) \equiv -\infty$  and  $x_{2^N}(t) = \infty$  for all  $t$ . In Eq.(3),  $\Delta$  is a small trim step (measured in volts). From the equation, we see that the entire trim operation only takes that unambiguous code  $b_{i-1}$  (see Fig.1) which is uniquely set to HIGH by the latch-bank logic at a time when  $v_{in}(t)$  falls into the quantization interval  $[x_{i-1}, x_i)$ . During the operation, two adjacent comparators with  $x_{i-1}$  and  $x_i$  are adapted simultaneously based on this code: the lower one is trimmed up and the higher trimmed down. An integrator, which takes the UP or DOWN trim step as its input signal, can thus accumulate the difference of the UP and DOWN trims for the  $(i-1)$ -th comparator block. The same adaptation applies to all the other comparator blocks.

Note that we have implicitly assumed a nearly-uniform amplitude distribution for the input signal  $v_{in}(t)$ . Therefore, the trimming process reaches its equilibrium when the occurrences of the UP and DOWN trims are approximately equal. At equilibrium, we expect that the initially-offset threshold  $x_i$  be at about the centre of its two neighbors  $x_{i-1}$  and  $x_{i+1}$ , i.e.,  $x_i = x_{i-1} + x_{i+1}$ . A small deviation due to the histogram nonuniformity finally remains as the convergence error with the trimmed thresholds. As long as the maximum deviation at equilibrium is within the resolution of the flash A/D converter,  $\pm 1/2$  LSB, there will be no chance that missing codes can occur.

As mentioned above, the assumption that we made for the self-trimming algorithm is that the input signal  $v_{in}(t)$  to the flash A/D converter has a stationary uniform distribution. This constrains the application of this technique to second-stage of a 2-step ADC [1] or A/D subconverters except the first of a pipelined A/D converter [2].

### III. FREQUENCY-DOMAIN ANALYSIS OF SELF-TRIMMING ALGORITHM

Generally, Eq.(1) can be approximately written as:

$$p(i, kT) = p(\text{code} = i - 1, \text{time} = kT) \\ \approx \overline{\rho(x_i, kT)} \cdot [x_i(kT) - x_{i-1}(kT)] + \overline{x_i(kT)} \cdot [\rho(x_i, kT) - \rho(x_{i-1}, kT)]$$

$$\text{where, } i = 0, \dots, 2^N + 1 \text{ and } k = 0, \dots, \infty \quad (4)$$

as shown in Fig.2. Some remarks need to be made about the equation as follows. The  $(2^N + 1)$ -th order PDF  $\rho(x, kT)$  in the equation is in general a continuous function of threshold variable  $x$  where  $x \in [0, V_{ref}]$ . To simplify the calculation of code histogram in the quantization interval

$[x_{i-1}(kT), x_i(kT))$  from Eq.(1), we use the average PDF  $\overline{\rho(x_i, kT)}$  for the quantization interval and

the average threshold  $\overline{x_i(kT)}$ , i.e.,  $\overline{\rho(x_i, kT)} = \frac{1}{x_i - x_{i-1}} \int_{x_{i-1}}^{x_i} \rho(x') dx'$  and

$$\overline{x_i(kT)} = \frac{(x_{i-1}(kT) + x_{i+1}(kT))}{2}. \text{ Under the strict-sense stationary (SSS) assumption on}$$

$x_i(kT)$ , these two terms - the average density of an stochastic SSS process and its mean remain unchanged with any time shift. It should also be noted that in the equation we have assigned  $i \in [0, 2^N + 1]$  rather than  $i \in [0, 2^N]$  for the code index  $i$  to account for the boundary conditions of various terms in the equation.

The average PDF  $\rho(x_i, kT)$  in the first term of Eq.(4) is positive real, and it together with a set of threshold variables  $x_i(kT)$  exists only over  $i \in [0, 2^N]$  and  $k \in [0, \infty)$ ; the boundary conditions for  $x_i(kT)$  in the equation are  $x_0(kT) \equiv 0$  (or say,  $x_0(kT) = -\infty$  because no codes are supposed to fall

into  $(-\infty, x_0(kT))$  in the ideal case), and  $x_{2^N}(kT) = V_{ref}$  (or say,  $x_{2^N}(kT) = \infty$  because no codes are supposed to fall into  $(x_{2^N}(kT), \infty)$  in the ideal case), and  $x_i(kT)$  can be set to zero for all  $i \notin [0, 2^N]$ , while the boundary conditions for  $\rho(x_i, kT)$  is set to zero for all  $i \notin [0, 2^N]$ . In general, the two terms  $\rho(x_i, kT)$  (or  $\rho(i, kT)$  for simplicity) and  $x_i(kT)$  are both the functions of the time variable  $k$  and the digital code index  $i$ .

The second term of Eq.(4),  $\overline{x_i(kT)} \cdot [\rho(x_i, kT) - \rho(x_{i-1}, kT)]$ , represents the contribution from the effect of the PDF nonuniformity. For a stationary uniform input signal  $v_{in}(kT)$ , this term vanishes as  $\rho(x_i, kT)$  is a constant  $\rho$  for all  $k$  and  $i$ .

### ANALYSIS OF 2-D ADAPTIVE SYSTEM UNDER UNIFORMITY ASSUMPTION OF INPUT'S PDF

Now we start to apply the 2-D z-transform that we introduced in [3] to Eq.(4), first to a case where  $\rho(i, kT) = \text{constant } \rho$  for all  $i$  and  $k$ , and then extend the results over to a nonuniform case. In the uniform case, the 2-D z-transform of Eq.(4) can be written as:

$$\begin{aligned}
 P(z_c, z_t) &= Z\{\rho \cdot (x_i(kT) - x_{i-1}(kT))\} \\
 &= Z\{\rho \cdot (\gamma_i(kT) - \gamma_{i-1}(k) + 1LSB)\} \\
 &= \rho \cdot \{(1 - z_c^{-1})\Gamma(z_c, z_t) + Z[1LSB]\} \quad , \text{ as } \gamma_{2^N}(kT) \equiv 0 \text{ for all } k \quad (5)
 \end{aligned}$$

where  $\Gamma(z_c, z_t) = Z\{\gamma_i(kT)\}$ . Our self-trimming algorithm updates its threshold variables  $x_i(kT)$  in a way similar to a sign-error stochastic LMS algorithm [5,6] by using a rule:

$$x_i(kT) = x_i(0) + g_i(kT)$$

$$g_i[(k+1)T] = B \cdot g_i(kT) + \mu \cdot e_i(kT), i = 0, \dots, 2^N + 1 \quad (6)$$

where  $e_i(kT)$  is in essence an instantaneous error signal reflecting the difference between the adapting value  $x_i(kT)$  and the desired value  $\hat{x}_i(kT)$  during the course of adaptation;  $\mu$  is a positive small-value parameter which controls the rate of convergence, and is proportional to the integrator gain  $\alpha$ ;  $B$  is a positive value close to unity, reflecting the constant leak rate of the integrator. In terms of INL  $\gamma_i(kT)$ , Eq.(6) can be rewritten as:

$$\begin{aligned} \gamma_i(kT) &= \gamma_i(0) + g_i(kT) \\ g_i[(k+1)T] &= B \cdot g_i(0) + \mu \cdot e'_i(kT) \end{aligned} \quad (7A)$$

where,

$$e'_i(kT) = e_i(kT) - \hat{e}_i(kT) \quad (7B)$$

$\hat{e}_i(kT)$  in the above equation is the error term in the ideal case; we expect that when  $x_i(kT) = \hat{x}_i(kT)$  and  $\rho(x_i, kT) = \rho(x_{i+1}, kT)$ ,  $\hat{e}_i(kT) = 0$  for all  $i$  and  $k$ .

In this study, we proposed a new definition for the error  $e_i(kT)$  corresponding to the mechanism of histogram smoothing (refer back to Eq.(3)):

$$e_i(kT) = W_{dn}p(i+1, kT) - W_{up}p(i, kT), i = 0, \dots, 2^N + 1 \quad (8)$$

where  $W_{dn}$  and  $W_{up}$  are two weighting coefficients (or say, weights) that correspond to our UP-DOWN trim operation, and are similar to the gradient signal (when the LMS algorithm is of the sign-data type) or the error signal (when the LMS algorithm is of the sign-error type) in the LMS algorithm. In practice, we can choose these two weights to be equal, i.e.,  $W_{dn} = W_{up} = W$ , and  $W$  is set to either 1 or 0 depending upon the digital output of  $i$ -th comparator. Eqs.(5)(6)(7)(8) together mathematically express the core idea of the self-trimming algorithm: to minimize pairwise the difference in the average numbers of digital

codes falling into the successive intervals by simultaneously setting the weights  $W_{dn}$  and  $W_{up}$  to either 1 or 0, and ultimately adjusting the corresponding thresholds  $x_i(kT)$  and  $x_{i+1}(kT)$ . In terms of  $\gamma_i(kT)$ , we can have  $e'_i(kT)$  as:

$$\begin{aligned} e'_i(kT) &= W_{dn}\rho[\gamma_{i+1}(kT) - \gamma_i(kT)] - W_{up}\rho[\gamma_i(kT) - \gamma_{i-1}(kT)] \\ &= W\rho[\gamma_{i+1}(kT) - 2\gamma_i(kT) + \gamma_{i-1}(kT)] , i = 0, \dots, 2^N + 1 \end{aligned} \quad (9)$$

The 2-D z-transform of  $e'_i(kT)$  is thus:

$$\begin{aligned} E'(z_c, z_t) &= W\rho \sum_{k=0}^{\infty} \sum_{i=0}^{2^N} [\gamma_{i+1}(kT) - 2\gamma_i(kT) + \gamma_{i-1}(kT)] z_c^{-i} z_t^{-k} \\ &= W\rho(z_c - 2 + z_c^{-1})\Gamma(z_c, z_t) \end{aligned} \quad (10)$$

as  $\Gamma(z_c, z_t) = Z\{\gamma_i(kT)\}$  and the two boundary conditions for the equations are:  $\gamma_0(kT) \equiv 0$  and  $\gamma_{2^N}(kT) \equiv 0$  for all  $k$ .

By applying the 2-D z-transform, Eq.(7) can be rewritten as:

$$\Gamma(z_c, z_t) = Z\{\gamma_i(0)\} + \frac{\mu}{z_t - B} E'(z_c, z_t) \quad (11)$$

Then we substitute Eq.(10) into Eq.(11). This thus finally leads to:

$$\Gamma(z_c, z_t) = Z\{\gamma_i(0)\} + \frac{\mu W\rho}{z_t - B} (z_c - 2 + z_c^{-1})\Gamma(z_c, z_t) \quad (12A)$$

and

$$H(z_c, z_t) = \frac{\Gamma(z_c, z_t)}{Z\{\gamma_i(0)\}} = \frac{z_t - B}{z_c - B - \mu W\rho(z_c - 2 + z_c^{-1})} \quad (12B)$$

It is interesting to see from Eq.(12) that the 2-D LMS system intrinsically behaves as a low-pass (LP) filter,

which is what we expected prior to this analysis. In this equation, the output  $\Gamma(z_c, z_t)$  (i.e., the 2-D z-transform of  $\gamma_i(kT)$ ) is the  $i$ -th threshold at time  $t = kT$ , and the input  $Z\{\gamma_i(0)\}$  the initial value of the  $i$ -th threshold which exists prior to the adaptation process. From Eq.(12A), we see that its second term on the right-hand-side (RHS),  $\frac{\mu W \rho}{z_t - B}(z_c - 2 + z_c^{-1})\Gamma(z_c, z_t)$ , represents the threshold nonuniformity of the comparator array, because  $(z_c - 2 + z_c^{-1}) = (z_c - 1)^2 z_c^{-1}$  estimates the second derivative. When all these thresholds of the flash A/D converter are perfectly aligned, i.e.,  $(z_c - 2 + z_c^{-1})\Gamma(z_c, z_t) = 0$  or  $x_i = (x_{i+1} + x_{i-1})/2$ , this term should perish. Otherwise, the second term is supposed to compensate the error portion of the initial threshold  $\gamma_i(0)$ .

## ANALYSIS OF 2-D ADAPTIVE SYSTEM

### UNDER ASSUMPTION OF INPUT'S NEARLY-UNIFORM PDF

In the above analysis, we have assumed the stationary uniformity of the PDF  $\rho$  that the stochastic input signal  $v_{in}(kT)$  should possess (i.e.,  $\rho(x_{i-1}, kT) = \rho(x_i, kT)$ ). Now let us consider the case when the uniformity assumption is replaced by a close-to-reality assumption that the threshold variable  $x(i, kT)$  varies much faster than  $\rho(x_i, kT)$  in the code domain  $i$ . Mathematically, this assumption can be stated as:

$$\left| \frac{x(i, kT) - [x(i-1, kT) + 1 \text{LSB}]}{x(i, kT)} \right| \gg \left| \frac{\rho(x_i, kT) - \rho(x_{i-1}, kT)}{\rho(x_i, kT)} \right| \quad (13)$$

From this assumption, we can readily derive  $\rho(x_i, kT) \gg \rho(x_i, kT) - \rho(x_{i-1}, kT)$  (because  $x(i, kT)$  or  $\rho(x_i, kT) > 0$  for all  $i$  and  $k$ ), i.e., this assumption implicitly asserts a nearly uniform PDF for  $v_{in}(kT)$ . In this case, we need to consider the second term of Eq.(4).

The following analysis is performed in the same way as above. First, we substitute Eq.(4) into Eqs.(7B) and (8), and then we have  $e'_i(kT)$  as:

$$\begin{aligned} e'_i(kT) \approx & W_{dn} \overline{\rho(x_{i+1}, kT)} [\gamma_{i+1}(kT) - \gamma_i(kT)] - W_{up} \overline{\rho(x_i, kT)} [\gamma_i(kT) - \gamma_{i-1}(kT)] \\ & + W_{dn} \overline{x_{i+1}(kT)} [\rho'(x_{i+1}, kT) - \rho'(x_i, kT)] - W_{up} \overline{x_i(kT)} [\rho'(x_i, kT) - \rho'(x_{i-1}, kT)] \end{aligned} \quad (14)$$

where the difference between the actual PDF  $\rho(x_i, kT)$  and the ideal PDF  $\hat{\rho}(\hat{x}_i, kT)$  is expressed as

$$\rho'(x_i, kT) = \rho(x_i, kT) - \hat{\rho}(\hat{x}_i, kT) .$$

From Eq.(13), we know that  $\rho(x_{i+1}, kT) \approx \rho(x_i, kT)$ . And also, we know by definition that  $\overline{x_{i+1}(kT)} \approx \overline{x_i(kT)} + 1LSB$ . By ignoring the effect of the term

$1LSB \cdot [\rho'(x_{i+1}, kT) - \rho'(x_i, kT)]$ , Eq.(14) can thus be approximately rewritten as (recall that

$$W_{dn} = W_{up} = W):$$

$$\begin{aligned} e'_i(kT) \approx & W \overline{\rho(x_i, kT)} [\gamma_{i+1}(kT) - 2\gamma_i(kT) + \gamma_{i-1}(kT)] \\ & + W \overline{x_i(kT)} [\rho'(x_{i+1}, kT) - 2\rho'(x_i, kT) + \rho'(x_{i-1}, kT)] \end{aligned} \quad (15)$$

The 2-D z-transform of Eq.(15) gives:

$$E'(z_c, z_t) \approx W \overline{\rho(x_i, kT)} (z_c - 2 + z_c^{-1}) \Gamma(z_c, z_t) + W \overline{x_i(kT)} (z_c - 2 + z_c^{-1}) \Psi'(z_c, z_t) \quad (16)$$

where  $\Gamma(z_c, z_t) = Z\{\gamma_i(kT)\}$  and  $\Psi'(z_c, z_t) = Z\{\rho'(x_i, kT)\}$  with a set of the boundary conditions:  $\gamma_0(kT) = 0$ ,  $\gamma_{2^N}(kT) = 0$ , and  $\rho'(x_0, kT) = 0$ ,  $\rho'(x_{2^N+1}, kT) = 0$  for all  $k$ .

By substituting Eq.(16) into Eq.(11), we can have:

$$\begin{aligned} \Gamma(z_c, z_t) &= Z\{\gamma_i(0)\} + \frac{\mu W}{z_t - B} \overline{\rho(x_i, kT)} (z_c - 2 + z_c^{-1}) \Gamma(z_c, z_t) \\ &\quad + \overline{x_i(kT)} (z_c - 2 + z_c^{-1}) \Psi'(z_c, z_t) \\ &= Z\{\gamma_i(0)\} + \frac{\mu W}{z_t - B} \overline{\rho(x_i, kT)} (z_c - 2 + z_c^{-1}) \Gamma(z_c, z_t) + \frac{\mu W}{z_t - B} \overline{x_i(kT)} \varepsilon \end{aligned} \quad (17A)$$

$$H(z_c, z_t) = \frac{\Gamma(z_c, z_t)}{Z\{\gamma_i(0)\} + \frac{\mu W}{z_t - B} \overline{x_i(kT)} \varepsilon} = \frac{z_t - B}{z_t - B - \mu W \overline{\rho(x_i, kT)} (z_c - 2 + z_c^{-1})} \quad (17B)$$

As in Eq.(12A), the first term of Eq.(17A) represents the input to the LP filter, while the second term the effect of the threshold nonuniformity. The third term  $\frac{\mu W}{z_t - B} \overline{x_i(kT)} \varepsilon$ , where

$\varepsilon = (z_c - 2 + z_c^{-1}) \Psi'(z_c, z_t)$ , of Eq.(17A) is proportional to the second derivative of  $\Psi'(z_c, z_t)$  in the code domain, reflecting the nonuniformity of the PDF  $\rho(x_i, kT)$ . When  $\varepsilon = 0$ , i.e., the PDF  $\rho(x_i, kT)$  is uniformly distributed, Eq.(17) is the same as the Eq.(12). It is worth noting here that both the equations end up with the error term  $(z_c - 2 + z_c^{-1}) \Gamma(z_c, z_t)$ , the 2-D z-transform of  $x_{i+1}(kT) - 2x_i(kT) + x_{i-1}(kT)$ , which is in essence equivalent to the instaneous error  $e_i(kT) = W_{dn} p(i+1, kT) - W_{up} p(i, kT)$  that this offset shaping algorithm is aimed at reducing on-line. In other words, we say that this offset shaping algorithm intrinsically takes  $e_i(kT) = x_{i+1}(kT) - 2x_i(kT) + x_{i-1}(kT)$  as its instaneous error.

The error term  $\frac{\mu W}{z_t - B} \overline{x_i(kT)} \varepsilon$  in Eq.(17A), which results from the PDF nonuniformity, is relatively very

small in amplitude when compared to  $\frac{\mu W}{z_t - B} \{ \overline{\rho(x_i, kT)} [z_c - 2 + z_c^{-1}] \Gamma(z_c, z_t) \}$  in the second term,

which results from the threshold nonuniformity (see [8] for discussion). We consider this third term,

$\frac{\mu W}{z_t - B} \overline{x_i(kT)} \varepsilon$ , as one of the noise sources together with the error-contaminated initial threshold

$Z\{\gamma_i(0)\}$ , thus both the terms being placed together in the denominator of Eq.(17B) and acting as the

target to be filtered out. Because the third term is relatively small under the assumption of a nearly-uniform

$\rho(x_i, kT)$  (seen from Eq.(13)), its effect on the spacing of the threshold array is negligible. But it can cause some problem by deviating the final equilibrium states of the threshold array somewhat from their desired values when the assumption given by Eq.(13) does not hold well. In practice, whether this small deviation is significant to the system's accuracy largely depends upon applications [8].

The system transfer function  $H(z_c, z_t)$  given by Eq.(17B) is not generally separable, i.e.,

$H(z_c, z_t) \neq H_1(z_c)H_2(z_t)$  for all  $z_c$  and  $z_t$ . This makes it difficult to determine the region of convergence of  $H(z_c, z_t)$  in the two dimensions. A comprehensive study of the 2-D stability problem is strongly required but it is beyond the scope of this paper.

### DE-COUPLING OF THE 2-D ADAPTIVE SYSTEM

For our A/D converter cases, however, the form of Eq.(17B) is fortunately simple: the coefficient  $\overline{\mu W \rho(x_i, kT)}$  of the term  $(z_c - 2 + z_c^{-1})$  in the denominator of this equation is in practice very small, and the term  $(z_c - 2 + z_c^{-1})$  itself is much smaller in amplitude than the inverse of  $\overline{\mu W \rho(x_i, kT)}$  (i.e.,

$$|z_c - 2 + z_c^{-1}| \ll \frac{1}{\overline{\mu W \rho(x_i, kT)}} \text{ ) when } z_c \text{-roots are not far from the unit circle in the } z_c \text{ domain.}$$

It is difficult to quantify the physical meaning of "very small" and "much smaller" or "not far" mentioned above. Therefore, let us consider some practical examples for these two terms  $\overline{\mu W \rho(x_i, kT)}$  and

$(z_c - 2 + z_c^{-1})$  instead. Assume a  $5\frac{1}{2}$ -bit flash A/D converter as the second stage of a 2-stage 10-bit A/D converter, of which the half-bit is reserved for digital error correction. As the digital error correction only needs two extra comparators to detect overflow and underflow of a residue from the first stage, the half-bit is actually just used to indicate the existence of these two comparators; therefore, this converter has 34

uniform quantization intervals (or LSBs) instead of 32, with one extra above the normal 32 intervals and the other below the normal intervals. Ideally, the averaged PDF  $\overline{\rho(x_i, kT)}$  is equal to  $\frac{1}{34}$  for all code  $i$  at all

time  $k$ . While the spacing of each quantization interval, 1 LSB, is set at

$\frac{5^{volt}(reference)}{34intervals} = 147.06mV$ , the adaptation step size  $\mu$  can thus be calculated as

$\frac{0.1mV(AdaptationStepSize)}{147.06mV} = 0.68 \times 10^{-3}$ . Therefore, the corresponding coefficient for the term

$(z_c - 2 + z_c^{-1})$  is  $\mu W \overline{\rho(x_i, kT)} = 2 \times 10^{-5}$  when  $W$  is set to 1. This tiny coefficient weights the term

$(z_c - 2 + z_c^{-1})$  so that some variation in this term, as long as the absolute value of this term is much

smaller than  $\frac{1}{\mu W \overline{\rho(x_i, kT)}} = 5 \times 10^4$ , has a negligible impact on the transfer function of the entire sys-

tem in the  $z_t$  domain.

The assumption that we have made above about the term  $(z_c - 2 + z_c^{-1})$  is in practice always valid for our

A/D converter cases. We can use the  $5\frac{1}{2}$ -bit A/D subconverter again as our example. For the subcon-

verter, the tolerable conversion error (up to which no missing codes occur) is  $\pm\frac{1}{2}LSB = \pm 73.53mV$ . In

current submicron CMOS technologies, well-designed comparators (with a DC supply of 5 volts) without any means of offset cancellation usually have random offsets as high as 100mV or so, and even higher when smaller device sizes are used. This is to say that the amplitude of random offsets in reality is usually around 1 LSB or somewhat higher. Now we need to extract a somewhat general idea about the  $z_c$ -roots of

the term  $(z_c - 2 + z_c^{-1})$  from the "real" numbers given above. Assuming that we have a  $5\frac{1}{2}$ -bit flash A/D

converter and the offsets of the converter, i.e., its successive thresholds  $x_i$  from their ideal values, are represented by a geometrically declining or increasing single-harmonic series  $\gamma_i = A\alpha^i \sin(\omega_c \Delta_c i)$ ,  $i = 0, \dots, 34$ . By z-transforming its periodic complex exponential in the code domain, we have:

$$\begin{aligned}
\Gamma(z_c) &= \sum_{i=0}^{34} \gamma_i z_c^{-i} \\
&= A \sum_{i=1}^{33} (\alpha e^{j(\omega_c \Delta_c)})^i z_c^{-i} \\
&= A \alpha e^{j(\omega_c \Delta_c)} z_c^{-1} [1 + \alpha e^{j(\omega_c \Delta_c)} z_c^{-1} + \dots + (\alpha e^{j(\omega_c \Delta_c)} z_c^{-1})^{32}] \quad (18)
\end{aligned}$$

The corresponding  $z_c$ -roots of  $\Gamma(z_c) = 0$  are:  $z_{c0(1, \dots, 31)} = \alpha e^{j(\omega_c \Delta_c + \frac{2\pi}{32}m)}$ , where  $m = 1, \dots, 31$ . These roots are all closely around the unit circle, and the distance between each root and the coordinate origin is determined by the damping factor  $\alpha$  which is in practice close to unity. It tends to be that even the peak of the series, either  $\alpha$  when  $\alpha \leq 1$  or  $\alpha^{33}$  when  $\alpha > 1$ , is not beyond a few LSBs. Let us set  $\alpha^{33}$  to be 10 LSB for example. We can find that in this case the maximum absolute value of the term  $(z_c - 2 + z_c^{-1})$  is less than 4, which is far smaller than that required by our assumption,  $5 \times 10^4$ . This conclusion can be extended over to a general INL series  $\gamma_i$  with some more mathematical complexity.

From the above discussion, we can see that the whole term  $\mu W \overline{\rho(x_i, kT)} (z_c - 2 + z_c^{-1})$  in Eq.(17) is almost idle in both the  $z_c$  and  $z_t$  domains. Therefore, we can de-couple Eq.(17) into a simple case, and then analyze the 2-D adaptive system approximately as given in the following sections.

#### IV. THE ADAPTIVE SYSTEM IN THE TIME DOMAIN

We can re-arrange Eq.(17A) as:

$$z_t \Gamma(z_c, z_t) - [B + \mu W \overline{\rho(x_i, kT)}(z_c - 2 + z_c^{-1})] \Gamma(z_c, z_t) = (z_t - B) Z\{\gamma_i(0)\} + \mu W \overline{x_i(kT)} \varepsilon \quad (19)$$

This is a first-order difference equation for the variable  $\Gamma(z_c, z_t)$ . We then consider the RHS term

$$(z_t - B) Z\{\gamma_i(0)\} + \mu W \overline{x_i(kT)} \varepsilon \quad \text{of the equation, as a whole, as the input to this differential system.}$$

Because of a relatively very small value of the term  $\mu W \overline{\rho(x_i, kT)}(z_c - 2 + z_c^{-1})$  compared to the constant leak rate  $B$ , the variable  $\Gamma(z_c, z_t)$  does not track the instantaneous fluctuation in the coefficient

$B + \mu W \overline{\rho(x_i, kT)}(z_c - 2 + z_c^{-1})$ . Similarly,  $\Gamma(z_c, z_t)$  also reacts very slowly to the change in the system input  $(z_t - B) Z\{\gamma_i(0)\} + \mu W \overline{x_i(kT)} \varepsilon$ . For this special case, we can obtain the "first"-order IIR system transfer function as:

$$H(z_c, z_t) = \frac{\Gamma(z_c, z_t)}{(z_t - B) Z\{\gamma_i(0)\} + \mu W \overline{x_i(kT)} \varepsilon} = \frac{1}{z_t - [B + \mu W \overline{\rho(x_i, kT)}(z_c - 2 + z_c^{-1})]} \quad (20)$$

This "first"-order LP filter has multiple poles (from multiple values of the variable  $z_c$ ) in the  $z_t$  plane at:

$$z_t = B + \mu W \overline{\rho(x_i, kT)}(z_c - 2 + z_c^{-1}) \quad (21)$$

It should be noted here that although Eq.(20) has a similar appearance as Eq.(17B), the physical interpretation of these two equations is conceptually different: the former is a special case of the bivariate system given by the latter under the two assumptions about  $\mu W \overline{\rho(x_i, kT)}$  and  $(z_c - 2 + z_c^{-1})$  discussed above.

The multiple poles in the  $z_t$  plane are determined by the  $z_c$ -roots of  $Z\{\gamma_i(kT)\} = 0$  at their desired

locations. These desired  $z_c$ -roots are all on the unit circle in the  $z_c$  plane (i.e., when  $\alpha$  in Eq.(18) is equal to unity and  $f_c$  equal to zero).

The location of these poles in the  $z_t$  plane can be illustrated by using the same  $5\frac{1}{2}$ -bit flash A/D converter as an example. Let us assume again that the offsets of such an A/D converter may be expressed by an INL sequence  $\gamma_i = A\alpha^i \sin(\omega_c \Delta_c i)$ ,  $i = 0, \dots, 34$ , where the damping factor  $\alpha$  is around unity. We expect that the final INL of the converter converges to  $\{\hat{\gamma}_i = \hat{A} \rightarrow 0, i = 0, \dots, 34\}$  with no harmonic distortion (i.e., when  $f_c = 0$ ). Since the desired frequency response of  $\{\hat{\gamma}_i\}$  can be considered as the reference input of the adaptive system given by Eq.(20), i.e.,  $Z\{\gamma_i\} = H(z_c, z_t)Z\{\hat{\gamma}_i\}$  where  $Z\{\gamma_i\}$  is the system output which reflects the converter's thresholds in a nonideal case and tracks the reference input,  $Z\{\hat{\gamma}_i\} = 0$  thus gives us a set of  $z_c$ -roots:  $\hat{z}_{c0(1, \dots, 32)} = e^{j\frac{2\pi}{33}m} = e^{j\theta}$ ,  $m = 1, \dots, 32$ .

These roots are equally spaced on the unit circle in the  $z_c$  plane, and set the multiple poles in the  $z_t$  plane as:

$$\hat{z}_{t(1, \dots, 31)} = B + \mu W \overline{\rho(x_i, kT)} (z_c - 2 + z_c^{-1}) \quad (22)$$

Because  $\mu$ ,  $W$  and  $\overline{\rho(x_i, kT)}$  are all positive real and their product is relatively very small compared to  $B$  (note that  $B \leq 1$ ), the second term in the above equation is always negative real. Therefore, these  $z_t$  poles are all located within the unit circle in the RHS of the  $z_t$  plane and all on the real axis adjacent to the left of the DC point  $z_t = 1$ , i.e., the adaptive system is stable in the time domain. The adaptive system thus functions as an LP filter to reduce high-frequency components of the INL sequence in the time domain. The frequency response of a self-trimming 2-bit flash A/D converter is given in Fig.3 as an exam-

ple.

**Fig.3 Frequency response of a self-trimming 2-bit flash A/D converter in time-frequency domain**

The special case that we consider in this section is the steady state of the system transfer function, i.e., the solution when  $z_t \rightarrow 1$  according to the Final Value Theorem for the steady-state response [7]. The physical interpretation of the steady state for our self-trimming flash A/D converter is that the frequencies of the UP and DOWN trims resulting from the digital output codes of the converter are equal. At such an equilibrium state, we have:

$$\frac{1}{z_t - B} = \frac{1}{1 - B} \text{ very large as } B \approx 1 \quad (23)$$

and thus the steady-state solution from Eq.(17A) is:

$$\Gamma(z_c) = Z\{\gamma_i(0)\} + \frac{\mu W}{1 - B} \overline{\rho(x_i, kT)} (z_c - 2 + z_c^{-1}) \Gamma(z_c) + \frac{\mu W}{1 - B} \overline{x_i(kT)} \varepsilon \quad (24)$$

Some simple manipulation of Eq.(24) finally leads to:

$$\Gamma(z_c) = \frac{-z_c \left[ Z\{\gamma_i(0)\} + \frac{\mu W}{1 - B} \overline{x_i(kT)} \varepsilon \right]}{\frac{\mu W \overline{\rho(x_i, kT)}}{1 - B} \left[ z_c^2 - \left( 2 + \frac{1 - B}{\mu W \overline{\rho(x_i, kT)}} \right) z_c + 1 \right]} \quad (25A)$$

and

$$H(z_c) = \frac{\Gamma(z_c)}{Z\{\gamma_i(0)\} + \frac{\mu W}{1-B} x_i(kT)\epsilon} \quad (25B)$$

Eq.(25B) is the  $z_c$  domain transfer function of a second-order LP IIR filter with a DC gain of unity, and has two poles in the  $z_c$  domain:

$$z_{c(1,2)} = \frac{2 + \zeta \pm \sqrt{\zeta^2 + 4\zeta}}{2}, \text{ where } \zeta = \frac{1-B}{\mu W \rho(x_i, kT)} \quad (26)$$

The absolute value of the parameter  $\zeta$  in the above equation is small around zero. When  $\zeta = 0$ , i.e.,  $B = 1$ , two poles are identically located at the DC point ( $z_c = 1$ ) of the unit circle. With another circle of  $\zeta$ , e.g.,  $\zeta = 2$ , we have:

$$z_{c(1,2)} = 2 \pm \sqrt{3}$$

These two poles are all on the real axis: one pole,  $z_{c1}$ , is outside the unit circle, while the other,  $z_{c2}$ , within the unit circle. Other choices of  $\zeta$  give poles which are located in the complex plane around  $z_c = 1$  of the unit circle.

Because of the finite extent of code variable  $i$ , the stability of the system in the  $z_c$  domain, i.e., whether the poles in the  $z_c$  domain are located within the unit circle, does not really matter to our concern. The matter that we are concerned about is that the stability problem in the  $z_c$  domain reflects the spacing of the threshold array  $x_i(kT)$ , because the poles given by the denominator of Eq.(25B) characterize the spacing. From Eq.(25B), we can see that the only parameter which affects the location of the poles is

$\zeta = \frac{1-B}{\mu W \overline{\rho(x_i, kT)}}$ , and thus  $\frac{1}{\mu W}$  since  $\overline{\rho(x_i, kT)}$  is the statistical average value and  $(1-B)$  is fixed

for certain integration circuitry.

Let us consider Eq.(25A) for the effect of the term  $\frac{1}{\mu W}$  as it resides in both the numerator and the denomi-

inator of the equation. The second term  $\mu W \overline{x_i(kT)} \varepsilon$  in the bracket of the numerator reflects the effect

from the PDF nonuniformity of the threshold array (recall that  $\varepsilon = (z_c - 2 + z_c^{-1})\Gamma(z_c, z_t)$ ). The effect

is additive to the initial value of the  $i$ -th threshold during the course of the threshold adaptation. The term

$\frac{1-B}{\mu W \overline{\rho(x_i, kT)}}$  in the bracket of the denominator solely determines the stability of the system in the  $z_c$

domain. Therefore, a good compromise is needed to make  $\frac{1}{\mu W}$  large enough so that the gain for the

noise  $\varepsilon$  is low while keeping  $\frac{1}{\mu W}$  small enough to ensure effective filtering (i.e., the poles in the  $z_c$  domain

are close to  $z_c = 1$ ) so that the final histogram has a good uniformity. As the feedback integrator tends to

be fixed, the adaptation step size  $\mu$  is actually the only controllable parameter for the term  $\frac{1}{\mu W}$ . For our

behavioral-level simulation, Eq.(25A) thus gives an important guideline in determining an appropriate value

of  $\mu$  for a large time frame: by decreasing  $\mu$ , we have a larger  $\frac{1}{\mu W}$  and thus a smaller final convergence

error; by increasing  $\mu$ , we have a smaller  $\frac{1}{\mu W}$  and thus faster convergence. This trade-off was demon-

strated in applications of the self-trimming technique to 2-step and pipelined multi-step A/D converters

[1,2].

It is worth noting that the parameter  $\frac{1}{\mu W}$  can be controlled in various ways. The approaches that we demonstrated in [1,2] are through a "direct" pulse control.

### References

- [1]. Z. Gu and W.M. Snelgrove, "A novel self-calibrating scheme for video-rate 2-step A/D converter", Proceedings of IEEE 1992 International Symposium on Circuits and Systems, Vol.2, pp601-604, San Diego, May 1992.
- [2]. Z. Gu and W. M. Snelgrove, "Application of a novel self-calibrating technique to pipelined multi-stage A/D converter", Proceedings of 35th Midwest Symposium on Circuits and Systems, Vol.1, pp64-67, Washington, DC., Aug.1992.
- [3]. Z. Gu and W. M. Snelgrove, "Frequency-Domain Analysis of A/D Converter Nonlinearity", submitted to IEEE 1994 International Symposium on Circuits and Systems, London, England, May 1994.
- [4]. J. Doernberg, H. S. Lee and D. A. Hodges, "Full-Speed Testing of A/D Converters", IEEE Journal of Solid-State Circuits, Vol.SC-20, No.6, pp1138-1143, Dec. 1985.
- [5]. R. T. Compton, Jr., "Adaptive Antenna: Concepts and Performance", Prentice Hall, 448pp, 1988.
- [6]. B. Widrow, P. E. Mantey, L. J. Griffiths, and B. B. Goode, "Adaptive Antenna Systems", Proc. of the IEEE, Vol.55, No.12, pp2143-2159, 1967.
- [7]. A. V. Oppenheim, A. S. Willsky and I. T. Young, "Signals and Systems", Prentice-Hall, 796pp, 1983.
- [8]. Z. Gu, "Self-Calibration Techniques for High-Speed A/D Converters: Analysis and Design", M.A.Sc Thesis, Dept. of Electrical and Computer Engineering, University of Toronto, Canada, 1993.